RING CURRENT AND INTERPLANETARY MEDIUM PARAMETERS

V. Yu. PISARSKIJ*), YA. I. FELDSTEIN**), N. M. RUDNEVA*), A. PRIGANCOVÁ***)

Резюме: *По среднечасовым данным рассмотрены параметр распада кольцевого тока и функция инжекции, связанная с условиями в межпланетной среде. Подчеркивается различие значений параметра распада в течение бури, зависящего от функции инжекции в период главной фазы и от DR вариации в фазе восстановления. Предложен алгоритм расчета магнитного поля кольцевого тока по параметрам межпланетной среды. Путем моделирования DR вариации для слабых и умеренных бурь, а также больших бурь продемонстрировано хорошее согласие модельных расчетов с данными наблюдений во время бурь.*

Summary: *Based on hourly averaged data, the ring current decay parameter and the injection function associated with interplanetary medium parameters are analysed. The distinction among the decay parameter values during a magnetic storm has been carefully drawn, the dependence of τ on the injection function during the main phase and on the DR variation during the recovery phase being emphasized. The modeling of the DR variation for weak and/or moderate storms as well as intensive storms carried out demonstrates a good agreement between the model time profiles and observed data of magnetic storm activity.*

1. INTRODUCTION

The ring current is one of major magnetospheric sinks of the solar wind energy input into the magnetosphere. Its development is due to the trapped radiation. Trapped particles undergo the azimuthal drift around the Earth at the distance of $3 \div 5$ Earth's radii, where the geomagnetic field is of a closed configuration. The injection of the solar wind plasma into the magnetosphere as well as the precipitation of energetic ionospheric particles into the ring current cause its intensification and, thereby, the occurrence of geomagnetic stroms. These abrupt magnetic disturbances, as a consequence of the superposition of the ring current magnetic field at the Earth's surface and the geodipole magnetic field, are of a global character. During the main phase of a magnetic storm, the geomagnetic field horizontal component decreases due the increasing ring current intensity. The field depression may reach hundreds of nT at the middle and low latitudes. It is followed gradually by the recovery phase of a geomagnetic storm, when the geomagnetic field returns to its previous level because of the loss of ring current particles. The growth rate and decay of the ring current reflect the energy balance in the solar wind – magnetosphere coupling. To study further these processes in terms of interplanetary medium parameters is of immense importance. The aim of this paper is to identify peculiarities of the ring current activity response to variable interplanetary parameters in order to model ring current magnetic field variations during geomagnetic storms of the different intensity.

*) Институт прикладной геофизики, Москва, СССР.
**) ИЗМИРАН, 142092 Москва, СССР.
***) Geophysical Institute, Slovak Acad. Sci., 842 28 Bratislava, Czechoslovakia

2. RING CURRENT MAGNETIC FIELD

2.1. DR variation

Variations of the ring current magnetic field observed at the Earth's surface are described by the energy balance relation as follows:

$$\mathrm{d}DR/\mathrm{d}t = F(t) - DR/\tau\,, \tag{1}$$

where $DR = Dst - bp^{1/2} + DCF_q$, Dst is a geomagnetic activity index, p is a solar wind dynamic pressure, b is the coupling coefficient between a solar wind pressure and ground effects of currents on the magnetopause, DCF_q is the magnetic field of currents on the magnetopause under magnetically quiet conditions, $F(t)$ is the injection function characterizing the energy input rate into the ring current, τ is a parameter of ring current decay characteristic time [1–4]. The expression (1) has been analysed on an hourly values time scale. The Dst values for each hour UT are given in [5], and interplanetary medium parameters necessary for the evaluation of p, DCF_q and $F(t)$ are given in [6]. Values of DCF_q were calculated for each month and the value of b was assumed to be constant and equal to 0·20 nT/(eV cm^{-3})$^{1/2}$.

The DR variation during a geomagnetic storm is defined by the relationship between $F(t)$ and DR/τ. The relation $|F(t)| > |DR/\tau|$ is valid for the storm main phase, and $|F(t)| < |DR/\tau|$ for the recovery phase. As far as $F(t)$ and DR/τ are concerned, values of $F(t)$ are associated with interplanetary medium parameters, and values of τ are related to intrinsic processes in the magnetosphere. Numerous studies have been carried out in order to define the relationship between the injection function $F(t)$ and interplanetary parameters (see the brief review in [7, 8]). It was found, on an hourly values time scale, $F(t)$ to depend on both the azimuthal component of the solar wind electric field and the IMF magnitude standard deviation [2, 9]. There have been devoted numerious investigations to the τ parameter determination during different epochs of a geomagnetic storm (see the brief review in [10]). Such an enhanced interest is caused by the fact that the total energy dissipation rate U_T inside the magnetosphere is to a considerable extent determined by the energy injection rate into the ring current related to U_{DR}, which in turn depends critically on the parameter τ: $U_{DR} = -0{\cdot}74 \times 10^{10}(\mathrm{d}DR/\mathrm{d}t + DR/\tau)$, W. The U_T values, being calculated with respect to different parameters of the solar wind, are obvious to use for comparison [3, 11 to 13]. The results of such a comparison make it possible to reveal the relation between the energy input into the magnetosphere and interplanetary medium parametrs [14]. Further progress in studying the relationship between the energy transferred into the magnetosphere and dissipation processes within it appears to be impossible without an accurate determination of the ring current decay parameter [15]. On the basis of hourly averaged data, there carried out the further investigation of both the τ parameter variations during different epochs of a geomagentic storm and the injection function $F(t)$, which describes the energy input rate into the ring current with respect to variable interplanetary conditions.

2.2. Modeling of the injection function

The injection function $F(t)$ has been shown to be dependent on the solar wind electric field azimuthal component [1, 2, 8, 9, 17] and also on the "viscous" friction between the solar wind and magnetosphere as well, which depends on the solar wind velocity [4, 8]. Then we have for $F(t)$:

$$F(t) = A_1 V(Bz - A_2\sigma) + A_3(V - 300) + A_4 , \tag{2}$$

where V is the solar wind velocity, Bz is the IMF north-south component, σ is the IMF magnitude variability, A_1, A_2, A_3 and A_4 are constant coefficients which have been determined by the method of stochastic approximation with adaptation [16]. In the model adopted, the τ parameter was assumed to be different during the geomagnetic storm epochs. The τ value during the main phase was considered to be constant as adopted in [17, 18]. During the recovery phase its value was considered to change freely with the ring current intensity. The method just mentioned was used to determine the τ parameter during the recovery phase $\tau_{\text{r.ph.}}$ under the assumption of the decay parameter during the main phase $\tau_{\text{m.ph.}}$ to be 4·9 h.

To choose the model parameters, there has been solved the problem of minimizing the functional of the quadratic misfit between observed values of DR (denoted as DR_{exp}) and those calculated by means of the model treated (denoted as DR_{mod}). The number of variables used for minimizing ranged from 9 to 25. The solution of the optimization problem of such multidimensional type is always a most complicated task because of computational difficulties. Another peculiarity of the problem tackled is of the kind that the fast converging methods of the gradient type fail when applied to this case.

2.3. Method of stochastic approximation

The features mentioned above were decisive in choosing the stochastic approximation method with adaptation in order to select appropriate values of the model parameters.

The vector of parameters U_{k+1} was calculated for the $(k+1)$th step as $U_{k+1} = U_k + \alpha\xi_k(\omega_k)$, where α is the co-ordinate step vector, and ξ_k is a vector of the random teaching process, which depends on the teaching vector ω_k. Components of the ω vector were re-evaluated using formulae:

$$\omega_{k+1}^i = \beta\omega_k^i - \delta\left[I(U_k) - I(U_{k-1})\right](U_k^i - U_{k-1}^i) ,$$
$$i = 1, \ldots, n ; \quad k = 1, 2, \ldots$$

where n defines the n-space where the optimization has been carried out, ω_k^i is the i-th component of the ω vector for the k-th iteration, I is a value of the quadratic misfit functional, and α, β, δ are constant parameters accepted.

If the values of ω_k^i with k increasing exceeded 1, the components were artificially made less in their absolute value. The vector ξ was calculated as $\xi(\omega) = (\eta + \omega)/|\eta + \omega|$, where η is a random vector with co-ordinates uniformly distributed in the interval $[-1, 1]$.

Thus, a displacement vector $\alpha_k \xi_k(\omega_k)$ has a determinate component at every step of the algorithm. The quicker this component increases the slower $I(U_k)$ decreases. At the same time, the stochastic component being present makes the method more flexible.

There have been carried out as many as 2000 ÷ 5000 iterations under the assumption of different initial approximation parameters U_0 and various displacement steps α. Finally, the obtained sets of optimal parameters of the *DR* model were compared. As a matter of fact, values obtained were close enough and the option of the best value of parameters analysed was really time-consuming for a computer.

2.4. Determination of the τ parameter

The relationship $F = DR_{\max}/\tau_{\text{m.ph.}}$ is valid for the maximum depression of the ring current magnetic field. The F value was calculated using Eq. (2), F leading $DR_{\max}$ by an hour. Then the $\tau_{\text{m.ph.}}$ parameters have been determined for 45 geomagnetic storms, for which the difference between DR variations in the adjacent two hours around $DR_{\max}$ is no more than 5%. It turned out the $\tau_{\text{m.ph.}}$ value to depend dramatically on F, just as in [3, 19].

For the more accurate determination of coefficients in Eq. (2) during the ring current main phase, 96 geomagnetic storms were analysed. There have been selected 227 two-hour intervals for which following conditions hold: $|\Delta Bz| < 2$ nT, $\Delta \sqrt{p} \leqq \leqq 10\,(\text{cV cm}^{-3})^{1/2}$, i.e. a *DCF* variation being less than 2 nT. Using the τ dependence on F, values of $F_{\text{exp}} = \mathrm{d}DR/\mathrm{d}t + DR/\tau$ were calculated for the intervals chosen. Finally, values of F_{exp} calculated have been compared with the injection function depending on the solar wind electric field azimuthal component defined as follows: BzV, $V(Bz - 0{\cdot}5\sigma)$, $V(Bz - 0{\cdot}67\sigma)$, $V(Bz - \sigma)$. The relation $V(Bz - 0{\cdot}67\sigma)$, being defined an hour before of the *DR* variation, turned out to be the best among all those mentioned above. In fact, the azimuthal component, evaluated using this relation an hour ahead of the ring current *DR* variations, gives the closest correlation with F_{exp}. For an illustration, Fig. 1a, b show the dependence of F_{exp} on BzV (Fig. 1a) and $V(Bz - 0{\cdot}67\sigma)$ (Fig. 1b), correlation coefficients being $r = 0{\cdot}83 \pm 0{\cdot}05$ and $r = 0{\cdot}88 \pm 0{\cdot}04$, respectively.

During the injection period which corresponds to the main phase of a geomagnetic storm, the injection function F_{mod}, governed by interplanetary medium parameters, can be expressed by means of Eq. (2) with specified coefficients as follows:

$$F_{\text{mod}} = 8{\cdot}2 \times 10^{-3} V(Bz - 0{\cdot}67\sigma) - 14{\cdot}1 \times 10^{-3}(V - 300) + 9{\cdot}4\,, \tag{3}$$

where F_{mod} is in nT/h, V is in km/s, Bz and σ are in nT. Figure 2 illustrates the relationship between F_{exp} and F_{mod} evaluated for 227 two-hour intervals mentioned above. The linear regression equation is shown graphically by the solid line, the correlation coefficient being equal to $0{\cdot}88 \pm 0{\cdot}05$.

The more accurate values of F_{mod}, obtained from Eq. (3), were used to calculate $\tau_{\text{m.ph.}}$ once more. The $\tau_{\text{m.ph.}}$ values were evaluated at the maximum ring current

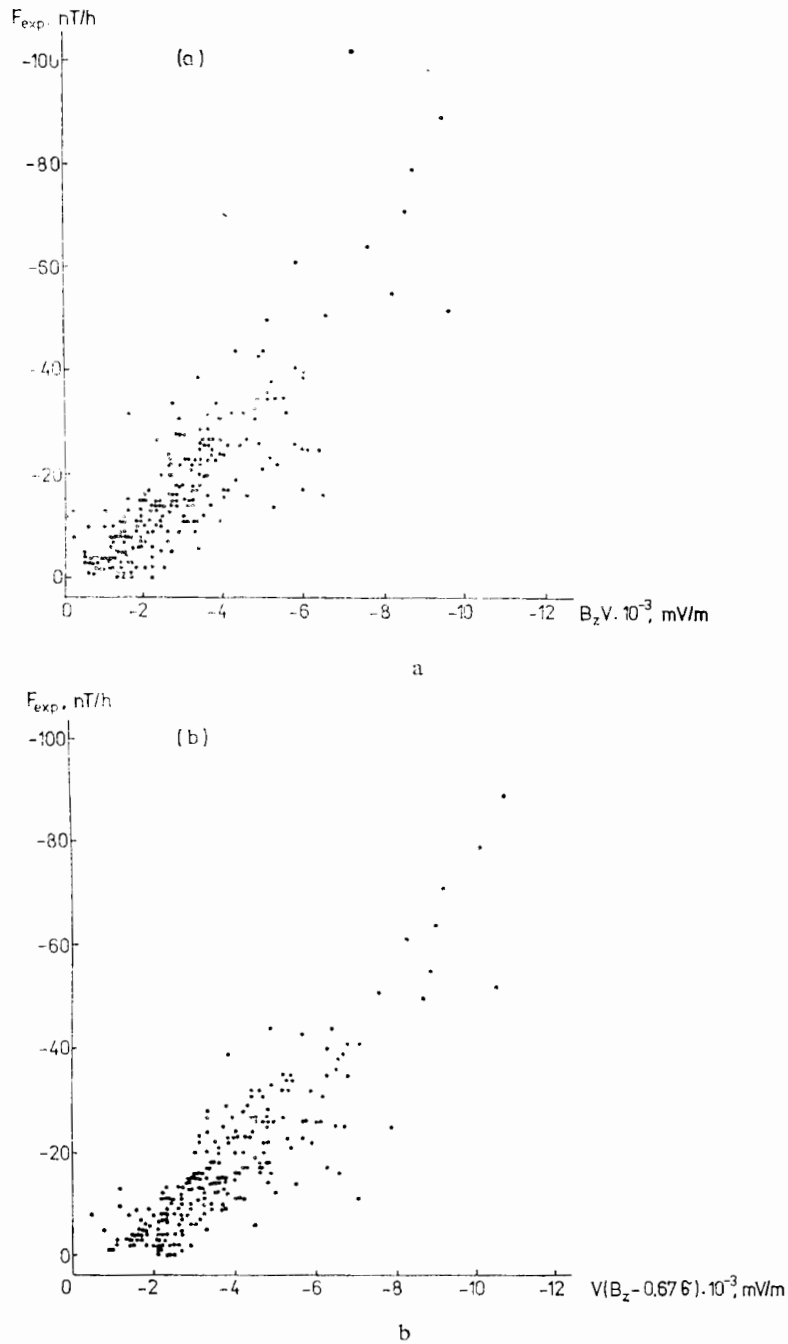

Fig. 1. Relationship between $F_{exp} = dDR/dt + DR/\tau$ and the solar wind electric field azimuthal component evaluated as BzV (a) and $V(Bz - 0{\cdot}67\sigma)$ (b), respectively, for 227 two - hour intervals during the injection period (the main phase) of a geomagnetic storm.

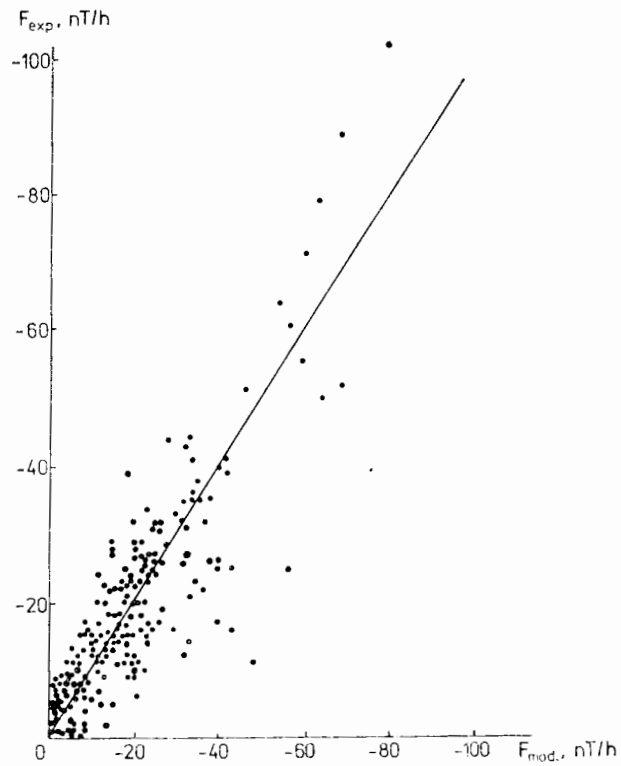

Fig. 2. Dependence of F_{exp} on F_{mod}. F_{mod} being calculated using Eq. (3) with an hour leading the corresponding variation of the ring current field.

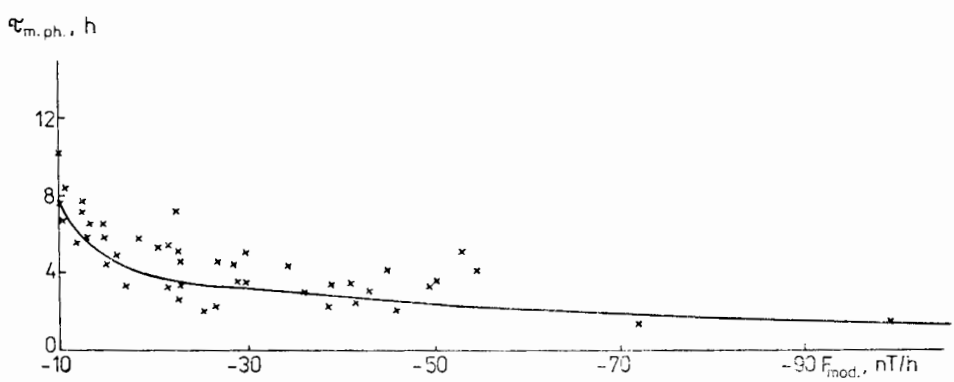

Fig. 3. Variations of the parameter τ due to F_{mod} during the injection period (the main phase) of a magnetic storm. Values of τ have been determined for the epoch of maximum intensity of 45 magnetic storms when values of DR for two adjacent hours near maximum differ by no more than 5% (crosses). The dependence of $\tau_{m.ph.}$ on F_{mod} for small and moderate storms adopted in model calculations is expressed by the solid line.

magnetic field intensity DR_{max} for 45 geomagnetic storms, with F_{mod} leading DR_{max} (Fig. 3). The solid line expresses the dependence of $\tau_{m.ph.}$ on F_{mod} adopted for model calculations of geomagnetic field variations during magnetic storms. It has been recognized earlier [8, 10] that there exists a certain difference between $\tau_{m.ph.}$ values for small and/or moderate storms as well as intensive storms, adopted in the analysis to come. The storms with $|DR_{max}| \geqq 160$ nT were chosen and values of $\tau_{m.ph.} = DR/(F - dDR/dt)$ were calculated for adjacent two-hour intervals. There is shown the relationship between $\tau_{m.ph.}$ and F_{mod} (Fig. 4) for 126 two-hour intervals analysed.

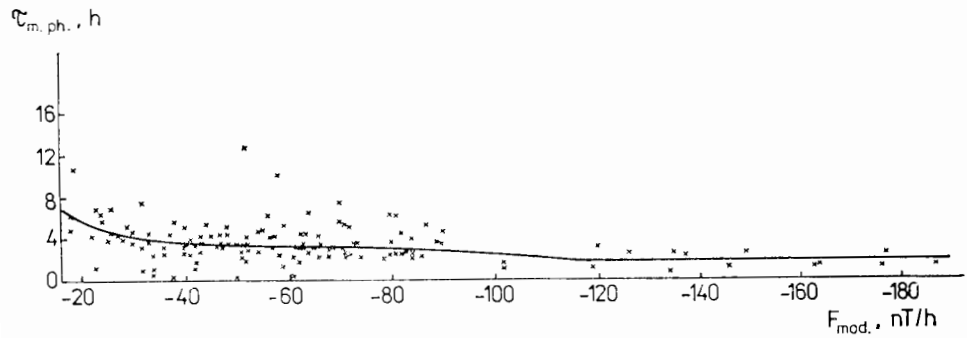

Fig. 4. Variations of parameter τ due to F_{mod} during the injection period of intensive magnetic storms. Values of τ were determined for the adjacent two-hour intervals using F_{mod} calculated by means of Eq. (3) an hour ahead (crosses). The dependence of $\tau_{m.ph.}$ on F_{mod} for intensive magnetic storms adopted in model calculations is expressed by the solid line.

The F_{mod} values were calculated using Eq. (3), with an hour ahead shift to the ring current magnetic field variations. The solid line in Fig. 4 expresses the dependence of $\tau_{m.ph.}$ on F_{mod} as assumed for the intensive storms modeling.

To divide a magnetic storm interval into the main phase (the injection period) and recovery phase (the decay period), we took into account the magnitude of the injection function. The portion of F_{mod} depending on the solar wind velocity appears to be present continuously. Keeping this fact in mind, we obtain the following condition for all hourly averaged data during the storm injection period:

$$8{\cdot}2 \times 10^{-3} V(Bz - 0{\cdot}67\sigma) - 14{\cdot}1 \times 10^{-3}(V - 300) + \\ + 9{\cdot}4 < -14{\cdot}1 \times 10^{-3}(V - 300)\,,$$

or

$$V(Bz - 0{\cdot}67\sigma) < -1146\,,$$

when the electromagnetic injection exceeds the viscous one. The remainding portion of a geomagnetic storm is attributed to the decay period in spite of the injection process into the ring current continues to proceed with the intensity:

$$-14{\cdot}1 \times 10^{-3}(V - 300) \quad \text{under the condition} \quad V > 300 \text{ km/s}\,.$$

As far as the parameter $\tau_{r.ph.}$ during the decay period (the recovery phase) is concerned, its values have been determined by the stochastic optimization method

mentioned above. For weak and/or moderate storms, $\tau_{r.ph.}$ increases when DR decreases, being ranged as follows:

$$\tau_{r.ph.} = \begin{cases} 5{\cdot}4\ \text{h}, & \text{if} \quad -150 \geqq DR \geqq -170\ \text{nT} \\ 9{\cdot}1\ \text{h}, & \text{if} \quad -30 \geqq DR \geqq -50\ \text{nT}. \end{cases}$$

For intensive storms, the $\tau_{r.ph.}$ values appear to be slightly dependent on DR, being ranged as follows:

$$\tau_{r.ph.} = \begin{cases} 10{\cdot}0\ \text{h}, & \text{if} \quad DR = -300\ \text{nT} \\ 10{\cdot}8\ \text{h}, & \text{if} \quad DR = -30\ \text{nT}. \end{cases}$$

The detailed pattern of $\tau_{r.ph.}$ variations can be found in Tab. 1. The $\tau_{r.ph.}$ values for intensive storms were calculated using 134 adjacent two-hour intervals. The scatter of values is quite considerable. But the corresponding median values are close to the $\tau_{r.ph.}$ dependent on DR as presented in Tab. 1. All results of the $\tau_{m.ph.}$ dependence on the injection function and $\tau_{r.ph.}$ dependence on ring current magnetic field variations, $\tau_{r.ph.}$ being obtained by means of the stochastic optimization method, are presented in Figs. 3, 4 and summarized in Tab. 1.

Table 1. Ring current decay parameters for magnetic storms of the different intensity: $\tau_{m.ph.}$, dependent on the injection function F during the injection period (the main physe) and $\tau_{r.ph.}$, dependent on DR during the decay period (the recovery phase)

Weak and moderate magnetic storms ($DR_{max} \geqq -160$ nT)				Intensive magnetic storms ($DR_{max} \leqq -160$ nT)			
$\lvert F\rvert$, nT/h	$\tau_{m.ph.}$, h	DR, nT	$\tau_{r.ph.}$, h	$\lvert F\rvert$, nT/h	$\tau_{m.ph.}$, h	DR, nT	$\tau_{r.ph.}$, h
4	11·5	$\geqq -10$	11·5	4	11·5	$\geqq -10$	11·5
6	10·2	$-10 \div -30$	10·2	6	10·2	$\div -30$	10·8
8	8·9	$-30 \div -50$	9·1	8	9·0	$\div -100$	10·5
10	7·6	$-50 \div -70$	8·0	10	8·0	-200	10·2
12	5·9	$-70 \div -90$	6·5	12	7·5	-300	10·0
14	5·0	$-90 \div -110$	6·3	14	7·0		
16	4·4	$-110 \div -130$	6·1	16	6·5		
18	4·1	$-130 \div -150$	6·0	18	6·0		
20	3·8	$-150 \div -160$	5·4	20	5·6		
25	3·4			25	4·8		
30	3·2			30	4·3		
40	2·8			40	3·8		
50	2·4			50	3·7		
60	2·1			60	3·6		
80	1·9			80	3·4		
100	1·7			100	2·4		
>100	1·7			>100	2·0		

3. COMPARISON OF STUDIES ON THE RING CURRENT MAGNETIC FILED MODELING

3.1. Injection function

It is of interest to compare the injection function suggested with those adopted earlier. The structure of the injection function reflects its duality: it is controlled by processes of reconnection of the interplanetary and geomagnetic fields (which is manifested by the dependence on both the IMF north-south component $Bz < 0$ and the IMF magnitude variability σ), and by viscous interaction between the solar wind and magnetosphere as well (which is manifested by the portion dependent on the solar wind velocity V). The injection into the ring current due to processes of reconnection has widely been discussed [1, 4, 7–9 and references therein]. The essential difference between Eq. (3) for the injection function and those given by other authors is just the presence of the additional injection due to the viscous interaction. In fact, the injection does not become zero during the northward IMF Bz component orientation, but some additional portion of the energy flux, dependent on the solar wind velocity, persists, increasing when V increases. Such an injection was already reported in [4]. It has been shown the injection function modul to increase by 1·9 nT/h due to the solar wind velocity enhancement from 300 km/s to 400 km/s.

There should be expected the decrease of the geomagnetic field level at the low-latitude observatories during the increased solar wind velocity as a direct result of viscous injection. Such a decrease was actually revealed during the night hours on the magnetically quiet days at several magnetic observatories in India [20]. The geomagnetic field level decreases by 10 nT as V increases by 100 km/s, the correlation coefficient being equal to $\sim 0{\cdot}6$. The decreasing of the Dst variation field by ~ 10 nT, caused by the solar wind velocity changing $\Delta V = 100$ km/s, has been revealed in intervals when the Earth meets high velocity solar wind streams [21]. The tendency of the horizontal component to decrease has also been observed at the Kakioka observatory during 22 magnetically quiet days with $Dst > 0$ under the condition of increasing solar wind velocity. In spite of quite large scatter of values, the increasing of the solar wind velocity by 100 km/s appears to cause the horizontal component decreasing by $5 \div 10$ nT. The magnitude of decreases varies from year to year, and $\Delta H/\cos \vartheta \doteq 10$ nT at the equator, ϑ being a geomagnetic latitude.

The ring current magnetic field decreases appear to be obvious when the Earth meets high velocity solar wind streams. Figure 5 shows hourly averaged values of DR evaluated during the $\geqq 5$ h long intervals with high velocity solar wind streams and the IMF Bz component exceeding 2 nT. There were analysed 36 such intervals chosen during the period of 1967–1970 [23]. The correlation coefficient between DR and V is $r = -0{\cdot}55$. According to the regression equation the solar wind velocity change $\Delta V = 100$ km/s causes $|\Delta DR| \doteq 15$ nT.

The portion of the injection function in (3), defining the viscous interaction, is quite

coincident with the magnetic field decreases at low-latitude observatories mentioned above. As a matter of fact, $\Delta F = -1{\cdot}41$ nT/h if $\Delta V \doteq 100$ km/s. This corresponds to $|\Delta DR| \doteq 13$ nT for quasi-stationary conditions if $\tau \doteq 9$ h is adopted. The viscous injection plays an important role in the ring current feeding during a final portion of the recovery phase. The best agreement between the observed ring current field and field values evaluated by DR modeling was obtained for $A_3 = -14{\cdot}1 \times 10^{-3}$ nT/(h . . km s^{-1}), namely, as accepted in (3).

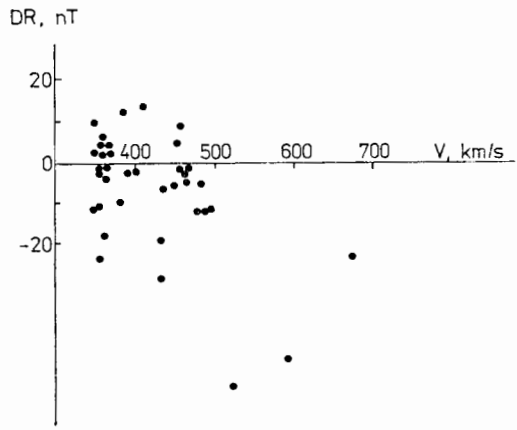

Fig. 5. Dependence of $DR = Dst - b\sqrt{p} + DCF_q$ on the solar wind velocity V when the Earth meets high velocity streams with the IMF north-south component $Bz > 0$.

The electromagnetic portion of the injection function together with the constant term (see Eq. (3)) quite likely has the structure suggested in [9], although the values of coefficients are distinctly different. It is caused by the different way of calculating F_{exp}. To calculate F_{exp} using data of 44 two-hour intervals, $\tau_{m.ph.}$ was assumed to be constant and equal to 6 h [9]. On the contrary, to calculate F_{exp}, used to determine the coefficients in (3), the dependence of $\tau_{m.ph.}$ on F_{mod} (Fig. 3) was taken into account.

3.2. Decay parameter

In this paper as in [3, 8, 10, 19], the parameter τ, which defines the particle dissipation rate for the ring current, is assumed to be different during the main phase (the injection period) and during the recovery phase (the decay period) of a geomagnetic storm. The $\tau_{m.ph.}$ variations due to F_{mod} are shown in Fig. 6. We can compare the relationship analysed for both weak and/or moderate (1) and intensive (2) storms. The value of $\tau_{m.ph.}$ adopted in [19] is also shown (3). For large values of the injection function, the value of $\tau_{m.ph.}$ drops down to 1·7 h or 2·0 h, which does not coincide with the value of 3 h according to [19]. In the range of the most frequent F_{mod} values ($-20 \div -80$ nT/h), the $\tau_{m.ph.}$ value adopted in [19] falls just between the curves (1) and (2) associated with storms of the different intensity. For the large F_{mod} values,

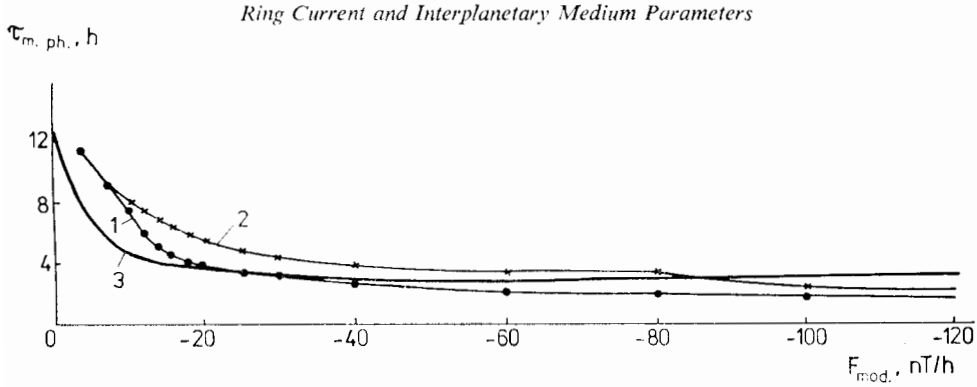

Fig. 6. Dependence of $\tau_{m.ph.}$ on F_{mod} for small and/or moderate (1) storms as well as intensive storms (2) according to results obtained in the paper. For comparison results of [19] (the curve 3) are also given.

we can see (Fig. 6) the decay parameter not to fall down to the value of 1 h or even less as claimed in [3]. Actually, such an abrupt decay $\tau < 1$ h means an enormously large energy injection rate into the ring current [24].

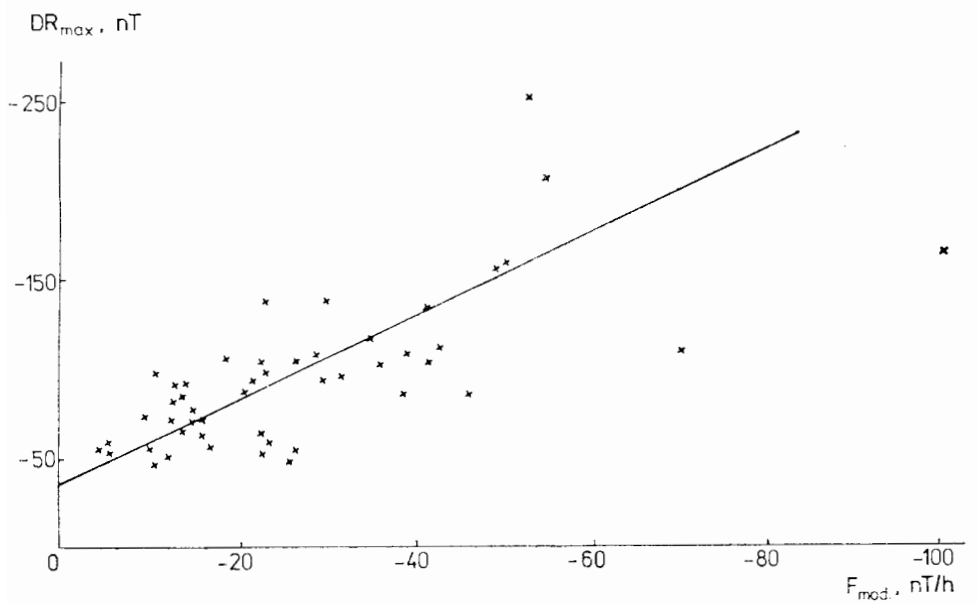

Fig. 7. Dependence od DR_{max} on F_{mod} valculated with an hour leading DR_{max}. The solid line represents the linear regression equation.

The assumption of $\tau_{m.ph.}$ to be dependent on the ring current magnetic field variations was adopted in [8, 10]. This dependence of $\tau_{m.ph.}$ on DR is statistically equivalent to the dependence of $\tau_{m.ph.}$ on F_{mod} which is strongly dependent on the solar wind electric field azimuthal component. In fact, there exists a distinct relation-

ship between the DR field intensity during the minima of the storm main phase (DR_{max}) and the solar wind electric field azimuthal component. The dependence of DR_{max} during the storm main phase on F_{mod} calculated, F_{mod} leading DR_{max} by an hour, is shown in Fig. 7. The values of F_{mod} were calculated by Eq. (3) using geomagnetic storm data for which DR variations during adjacent two-hour intervals near DR_{max} differ by no more than 5%. The linear regression equation reads as follows:

$$DR_{max}^{(i)} = (2{\cdot}35 \pm 0{\cdot}21)\, F_{mod}^{(i-1)} - (35{\cdot}0 \pm 6{\cdot}9), \tag{4}$$

the correlation coefficient being $r = 0{\cdot}69 \pm 0{\cdot}21$. If there were a functional linear dependence of DR_{max} on F_{mod} it would have meant the value of τ to be constant during the main phase. Such an assumption was adopted in [17, 18], and $\tau_{m.ph.}$ was supposed to be equal to 6 h. However, there is an essential scatter as far as the linear dependence of $\tau_{m.ph.}$ on F_{mod} is concerned. It means that $\tau_{m.ph.} \neq$ const as shown above. In fact, the relationship between F_{mod} and DR is most likely to exist in

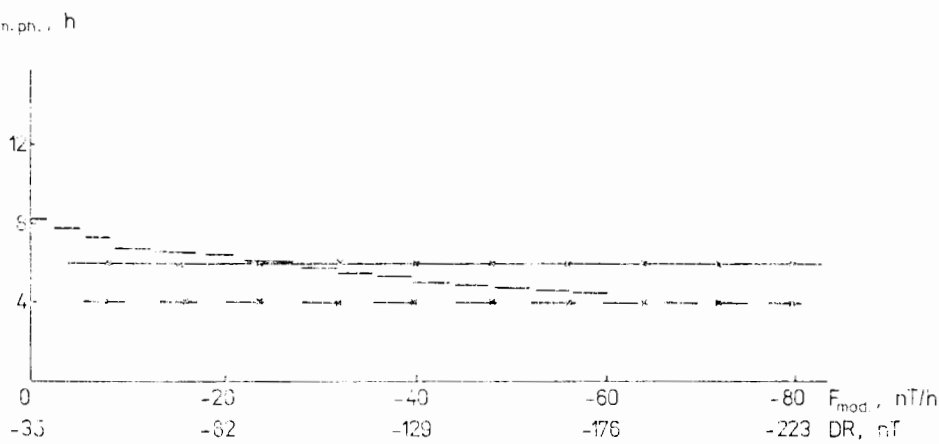

Fig. 8. The decay parameter during a magnetic storm main phase in terms of DR according to [18] — a solid line with crosses, [9] — a dashed line with crosses, and [10] — a dashed line. The F_{mod} scale was recalculated using Eq. (4).

the first approximation, i.e. the more intensive the injection, the more distinct the following decrease of the geomagnetic field due to the ring current magnetic field variations. The dependence of $\tau_{m.ph.}$ on DR [10] can then be re-evaluated into the dependence of $\tau_{m.ph.}$ on F_{mod}. The recalculated values have been used for the construction of Fig. 8, in which two scales for the abscissa are shown, DR and F_{mod} being related according to Eq. (4). The dependence of $\tau_{m.ph.}$ on DR adopted in [10] (a dash-and-dash line) can be seen, the $\tau_{m.ph.}$ decreases due to the intensified injection being not so essential as in Fig. 3. The values of $\tau_{m.ph.} = 6$ h and $\tau_{m.ph.} = 4$ h (a solid line with crosses and a dashed line with crosses, respectively) adopted in [18] and [9], respectively, are shown for comparison as well.

The determination of $\tau_{r.ph.}$ makes some difficulties discussed in detail in [10]. There are some discripancies as far as the dependence of $\tau_{r.ph.}$ on DR is concerned. According to [9, 17, 18], the increasing of $\tau_{r.ph.}$ due to the $|DR|$ growth is evident. The increasing of $\tau_{r.ph.}$ caused by decreasing $|DR|$ has also been reported [8, 10]. In our opinion, the increasing of $\tau_{r.ph.}$ due to the $|DR|$ decreasing during an individual storm seems to be more natural as it reflects a faster loss of shortlived particles, i.e. the ring current destruction which begins from its innermost shells around the Earth. At the same time, different types of storms are characterized by specific dependences of $\tau_{r.ph.}$ on DR. The $\tau_{r.ph.}$ values for intensive storms exceed essentially those for weak and/or moderate storms as can be seen in the Tab. 1. The expressions for the $\tau_{r.ph.}$ dependence on DR_{max} defining the maximum depression of the geomagnetic field during the main phase have been found [9, 17, 18, 19]. The amount of points, used to obtain the statistical linear relationship between $\tau_{r.ph.}$ and DR_{max}, was

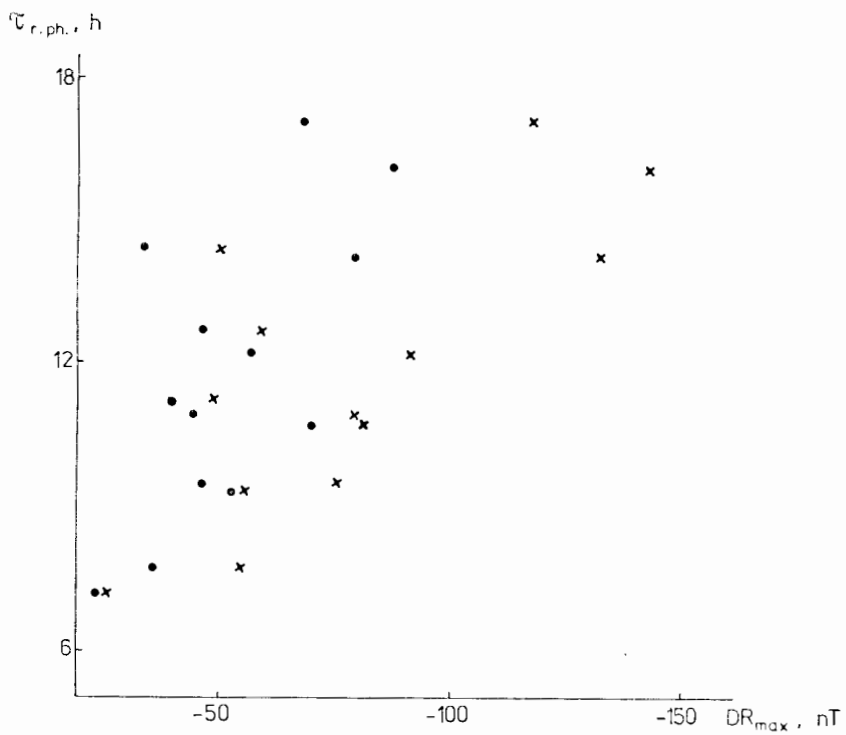

Fig. 9. Dependence of $\tau_{r.ph.}$ on DR_{max} according to [17] (crosses). Dots correspond to the same values of $\tau_{r.ph.}(DR)$ after IMF northward turnings.

limited and rather scattered. For this reason, there is no surprise that a slight change in the way of selecting magnetically quiet intervals during the storm recovery phase has caused the essential change in the relation analysed. According to [17, 19] we have for example:

$$\tau_{\text{r.ph.}} = 3{\cdot}6 \pm 0{\cdot}09|DR_{\max}|\,, \quad [18]$$

$$\tau_{\text{r.ph.}} = 6{\cdot}6 \pm 0{\cdot}07|DR_{\max}|\,, \quad [9, 19]\,.$$

The relation of $\tau_{\text{r.ph.}}$ to $DR_{\max}$ (crosses) evaluated [17, 19] for 13 geomagnetic stroms during intervals with $Bz > 0$ and $\sigma \leqq |Bz|$ is shown in Fig. 9. To calculate $\tau_{\text{r.ph.}}$ by the DR modeling, the DR values after the end of the injection in the ring current were used instead of $DR_{\max}$ [9, 19]. In such a case, the values of DR and $DR_{\max}$ sometimes differ dramatically. In Fig. 9. the same values of $\tau_{\text{r.ph.}}$ and corresponding DR values for the very hour of the IMF northward turning are presented by dots. The tendency of $\tau_{\text{r.ph.}}$ to increase as $|DR|$ increases becomes less distinct in this case. The scatter of dots becomes expressive, the regression line slope being increased by 1·5 times.

4. MODELING OF DR VARIATIONS

To calculate the ring current magnetic field variations the algorithm was constructed on the basis of the previous analysis using the recurrent relationship:

$$DR^{(i)} = \left(DR^{(i-1)}(2 - 1/\tau) + 2F_{\text{mod}}^{(i-1)}\right)/(2 + 1/\tau)\,,$$

where the injection function F_{mod} was evaluated as follows:

$$F_{\text{mod}} = \begin{cases} 8{\cdot}2 \times 10^{-3} V(Bz - 0{\cdot}67\sigma_k) - 14{\cdot}1 \times 10^{-3}(V - 300) + 9{\cdot}4\,, \\ \quad \text{if} \quad V(Bz - 0{\cdot}67\sigma_k) < -1146 \quad \text{(the injection period)} \\ -14{\cdot}1 \times 10^{-3}(V - 300)\,, \\ \quad \text{if} \quad V(Bz - 0{\cdot}67\sigma_k) > -1146 \quad \text{(the decay period)}\,, \end{cases}$$

where the IMF magnitude standard deviation σ_k is:

$$\sigma_k = \begin{cases} \sigma\,, & \text{if} \quad \sigma \geqq 6\ \text{nT} \\ 0\,, & \text{if} \quad \sigma < 6\ \text{nT}\,. \end{cases}$$

The expression for determining of the injection function is the same for all storms regardless of their intensity. The separate values of the decay parameter τ were adopted for the main and recovery phases, $\tau_{\text{m.ph.}}$ being considered in terms of F during the injection period and $\tau_{\text{r.ph.}}$ being considered in terms of DR during the decay period. The values of τ for weak and/or moderate storms ($DR_{\max} \leqq -150 \div -160$ nT) and intensive storms ($DR_{\max} > -150 \div -160$ nT) were used as given in Tab. 1.

The DR_{mod} values for 96 selected intervals were evaluated using the algorithm mentioned above. The intervals were selected during the period of 1967–1980 under the condition of Dst field decreases to be by 60 nT or more. The DR_{mod} values calculated were compared with observed ring current magnetic field variations DR_{exp}.

It is worthwhile to note that the mean hourly value standard deviation of DR_{mod} relative to DR_{exp} is 14 nT for the whole amount of data analysed (5352 hours). The DR_{exp} (observed ring current activity data) and DR_{mod} (model ring current magnetic

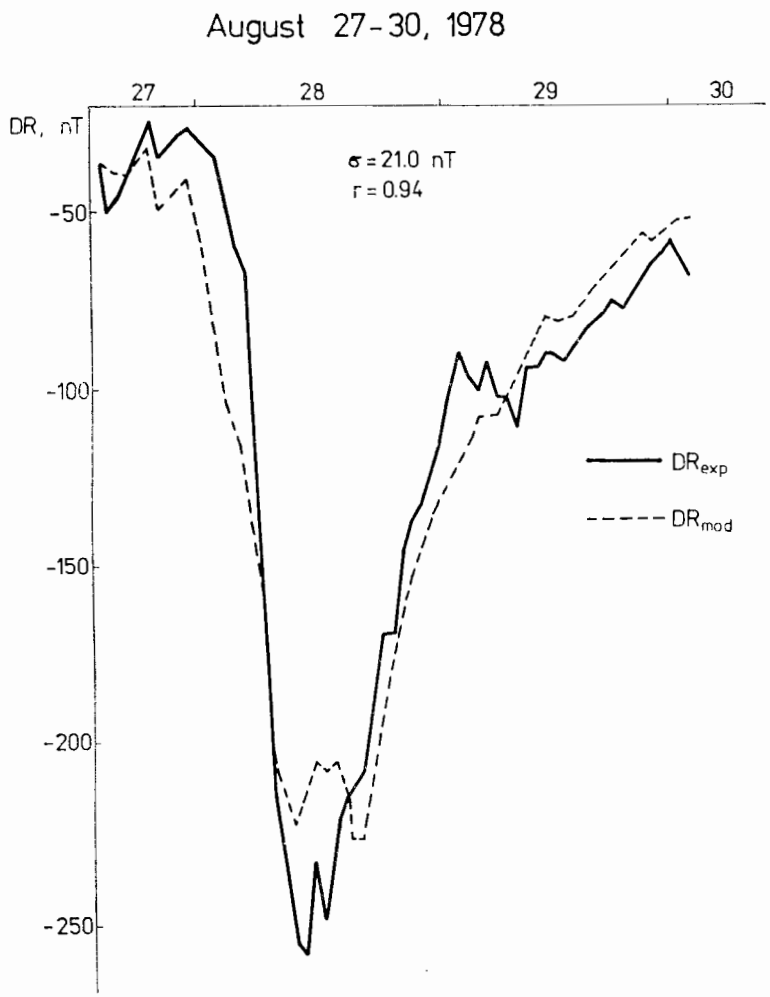

Fig. 10a. Modeling of the DR variation for the August 27—30, 1978 magnetic storm.

field variations) time profiles are plotted in Fig. 10 for comparison. Three intensive (Fig. 10, a—c) and three moderate storms (Fig. 10, d—f) were chosen for the illustration. Correlation coefficients r between DR_{exp} and DR_{mod} as well as mean square deviations σ referred to an hourly value in the interval analysed are given in Fig. 10 for all storms illustrated. A good agreement between the model time profiles and observed field variations is clearly seen.

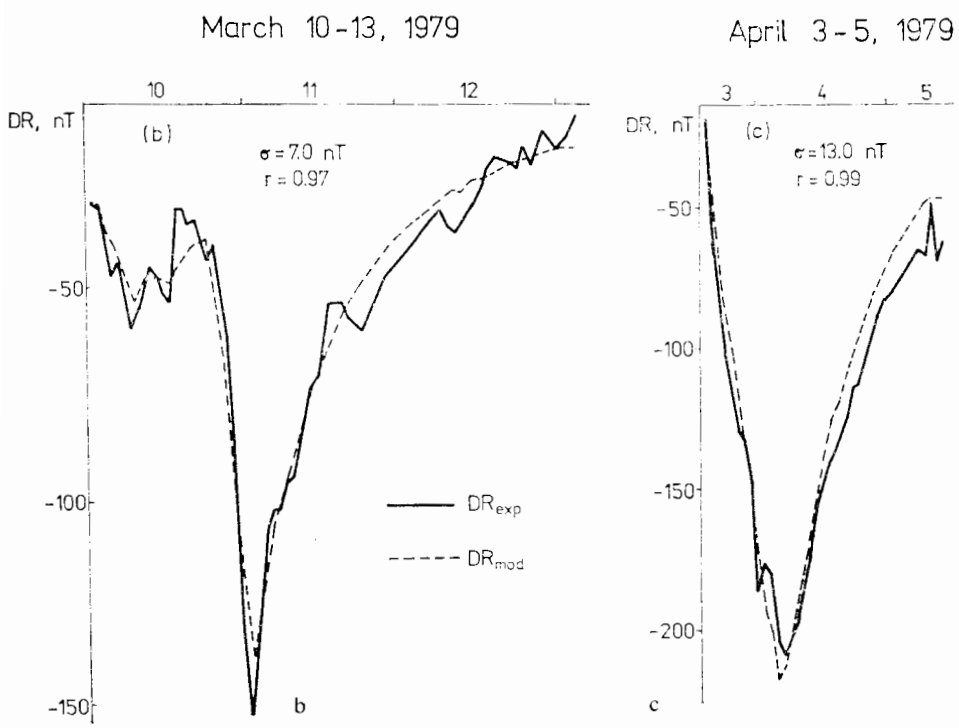

Fig. 10b, c. As for Fig. 10a but for the March 10—13, 1979 (b) and April 3—5, 1979 (c) magnetic stroms.

5. DISCUSSION AND CONCLUSION

The successful modeling of the ring current magnetic field variations infers the necessity to analyse properly the energy injection rate into the ring current, associated with interplanetary medium parameters. The injection is assumed to carry out in two principal ways. Processes associated with the viscous interaction of the solar wind and the magnetosphere are controlled by the solar wind velocity. On the other hand, processes of reconnection of the interplanetary and geomagnetic fields are controlled by the IMF north-south component $B_z < 0$ and the IMF magnitude variability. Such versatility of governing parameters makes difficulties as to an adequate identification of the injection function. Moreover, the ring current decay parameter is used to be different during a geomagnetic storm, its values being specific for the main and recovery phases. Finally, decay parameter values during the injection period (the main phase) are controlled by the injection function and its values during the decay period (the recovery phase) are governed by the ring current magnetic field variations. From the view-point of physical processes taking place in the ring current belt, the character of the τ parameter variations during different storm phases reflects

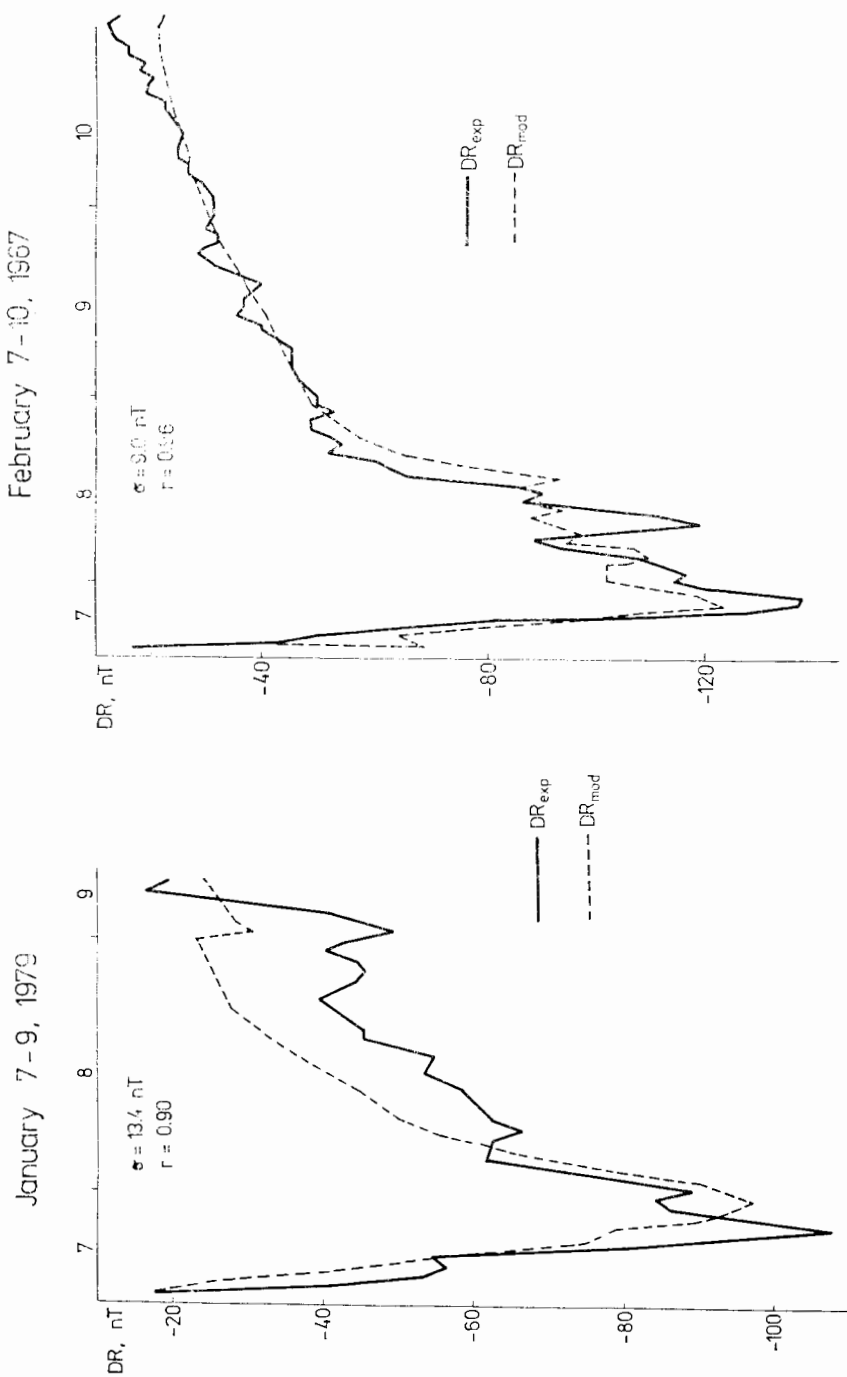

Fig. 10d. As for Fig. 10a but for the January 7–9, 1979 magnetic storm.

Fig. 10e. As Fig. 10a but for the February 7–10, 1967 magnetic storm.

the fundamental difference in the plasma loss processes. These processes are much faster during the storm main phase than during the recovery phase, the decay parameter being smaller during the injection period. It means that just trapped particles are detained in the geomagnetic field for a shorter time than particles which have not escaped during few hours. Furthermore, the decay parameter τ is different for weak

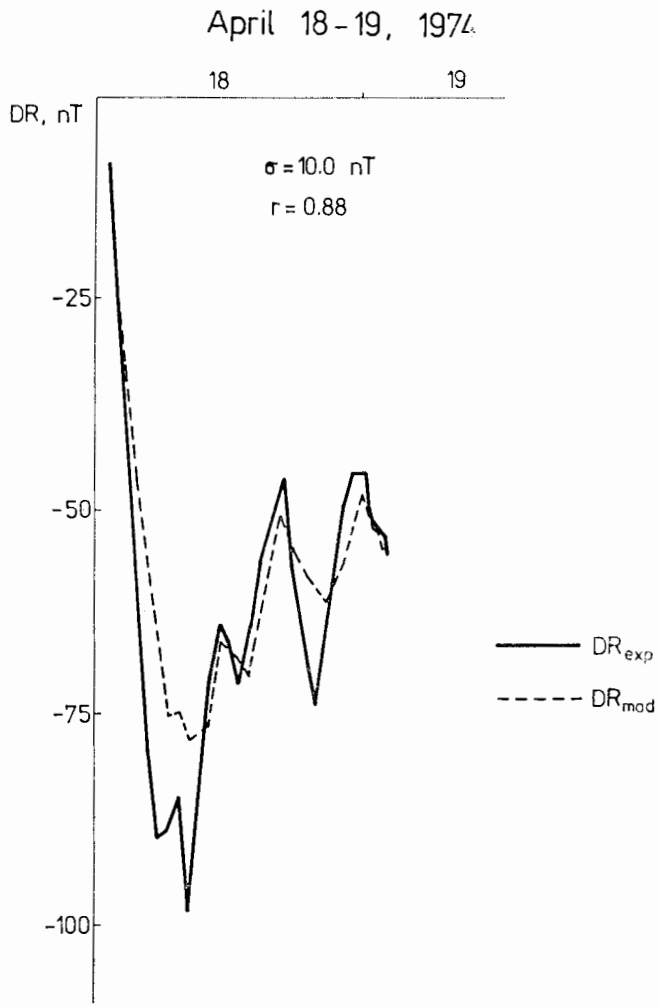

Fig. 10f. As for Fig. 10a but for the April 18—19, 1974 magnetic storm.

and/or moderate storms as well as intensive storms. This fact is partly caused by the ring current location in the magnetosphere. However, the main reasons for this difference are both the fluctuations of the chemical composition as to ring current ions and their varying energetic characteristics. The slower ring current decay process during the recovery phase of intensive storms testifies such association.

Taking into account the decay parameter distinction for different phases of a geomagnetic storm and the dependence of the injection function on interplanetary parameters, the algorithm was constructed for the modeling of ring current magnetic field variations. The observed ring current activity and model time profiles reveal a good agreement for both weak and/or moderate storms and intensive storms. Therefore, we may consider the results obtained as further evidence for the adequate identification and accurate understanding of the solar wind – magnetosphere coupling mechanism.

Received 21. 10. 1987 *Reviewer: L. Třísková*

References

[1] R. K. Burton, R. L. McPherron, C. T. Russell: An empirical relationship between interplanetary conditions and *Dst*, J. Geophys. Res., 80 (1985), 4204.

[2] М. С. Бобров: Параметры солнечного ветра, отверственные за инжекцию плазмы в область магнитосферного кольцевого тока, Астр. ж., 54 (1977), 1335.

[3] S. I. Akasofu: Energy coupling between the solar wind and the magnetosphere, Space Sci. Reviews, 28 (1981), 121.

[4] Y. I. Feldstein, V. Yu. Pisarskij, N. M. Rudneva, A. Grafe: Ring current simulation in connection with interplanetary space conditions, Plan. Space Sci., 32 (1984), 975.

[5] IAGA Bulletin N 32, Geomagnetic Data. Int. Union Geod. Geoph., Paris.

[6] J. H. King: Interplanetary medium data book, Suppl. 1, (1979) and Suppl. 2 (1983), NSSDC, NASA.

[7] T. Murayama: Coupling function between solar wind parameters and geomagnetic indices, Rev. Geoph. Space Phys., 20 (1982), 623.

[8] В.Ю. Писарский, Н. М. Руднева, Я. И. Фельдштейн, Н. Г. Ворфоломеева, А. Графе: Моделирование геомагнитного эффекта кольцевого тока по среднечасовым параметрам межпланетной среды. Препринт № 19 (552), ИЗМИРАН, М., 1985.

[9] М. И. Пудовкин, С. А. Зайцева, Л. З. Сизова, Н. М. Орлова: Вариации поля *Dst* в зависимости от параметров солнечного ветра. Геом. и Аэрон., 25 (1985), 812.

[10] В. Ю. Писарский, Н. М. Руднева, Я. И. Фельдштейн, А. Графе: О параметре распада кольцевого тока. Препринт № 20 (553), ИЗМИРАН, М., 1985.

[11] D. N. Baker, R. D. Zwickl, S. J. Bame, E. W. Hones, B. T. Tsurutani, E. J. Smith, S. I. Akasofu: An ISEE – 3 high-time resolution study of interplanetary parameter correlations with magnetospheric activity, J. Geoph. Res., 88 (1983), 6230.

[12] S. I. Akasofu, C. Olmsted, E. J. Smith, B. T. Tsurutani, R. Okida, D. N. Baker: Solar wind variations and geomagnetic storms: a study of individual storms based on high time resolution ISEE data, J. Geoph. Res., 90 (1985), 325.

[13] Y. I. Feldstein, A. E. Levitin, V. Yu. Pisarskij, N. M. Rudneva, A. Grafe, P. Ochabová, A. Prigancová: Energy regimes in the Earth's magnetosphere. Studia geoph. et geod., 30 (1986), 268.

[14] D. N. Baker, L. F. Bargatze, R. D. Zwickl: Magnetospheric response to the IMF. Substorms. J. Geom. Geoel., 38 (1986), 1047.

[15] S. I. Akasofu: Some critical issues on magnetospheric substorms. Plan. Space Sci., 34 (1986), 563.

[16] Ф. П. Васильев: Численные методы решения экспериментальных задач. Наука, М., 1980.

[17] M. I. Pudovkin, S. A. Zaitseva, L. Z. Sizova: Growth rate and decay of magnetospheric ring current. Plan. Space Sci., 33 (1985), 1097.

[18] Л. З. Сизова, С. А. Зайцева: Скорость роста и распада кольцевого тока. Сб. Геомагнитные вариации и солнечный ветер (А. И. Лаптыхов, ред.) ИЗМИРАН, М., 1984.

[19] М. И. Пудовкин, А. Графе, С. А. Зайцева, Л. З. Сизова, А. В. Усманов: Расчет поля *Dst* — вариации по параметрам солнечного ветра. Препринт № 60 (593),ИЗМИРАН, М., 1985.

[20] G. K. Rangarajan: Long and short term relationships between solar wind velocity and geomagnetic field at low latitudes. Proc. Indian Ac. Sci. (Earth Planet. Sci.), 93 (1984), 343.

[21] Л. П. Щадрина, Я. И. Плотников: Два типа бурь и передача энергии солнечного ветра. Симпозиум „Высокоширотные магнитные явления". Тезисы докладов, Суздаль, 1986.

[22] Ц. Д. Порчхидзе, Л. Кизирия, В. Ю. Писарский, Н. Г. Ворфоломеева, Ю. Р. Ривин, Я. И. Фельдштейн: Магнитное поле на низкоширотных обсерваториях в магнитно-спокойные дни. Сб. ИЗМИРАН, 1987.

[23] В. Ю. Писарский, Н. М. Руднева: Характеристики солнечного ветра и межпланетного магнитного поля в 1967 – 1977 гг. Каталог высокоскоростных потоков солнечного ветра, ИПГ, М., 1986.

[24] D. P. Stern: Energetics of the magnetosphere. Space Sci. Rev., 39 (1984), 193.